Cellular Signaling and Protein−Protein Interactions Studied Using Fluorescence Recovery after Photobleaching†

Star M. Dunham,[§,‡] Haridas E. Pudavar,[‡] Paras N. Prasad,*[,‡] and Michal K. Stachowiak[§]

Molecular and Structural Neurobiology and Gene Therapy Program, Department of Pathology and Anatomical Sciences, Farber Hall 206A, State University of New York at Buffalo, 3435 Main Street, Buffalo, New York 142214, and Institute for Lasers, Photonics and BioPhotonics, 428, NSC, Department of Chemistry, State University of New York at Buffalo, Buffalo, New York 14260

Received: February 4, 2004; In Final Form: March 29, 2004

Transduction of intracellular signals requires multiple protein−protein and cellular structure interactions. These interactions affect the mobility of the involved proteins; therefore mobility measurements could provide insight into these interactions. Fluorescence recovery after photobleaching (FRAP) is an effective tool to analyze intracellular protein mobility. In the present study we report the application of FRAP to monitor intracellular signaling by fibroblast growth factor receptor (FGFR1), a transmembrane and a nuclear protein. FGFs have been shown to stimulate phosphatidyl inositol 3-kinase (PI3K) activity through activation of a high affinity FGFR. The interaction of FGFR1 phosphotyrosines with the regulatory subunit, p85α, of PI3K has been indicated by FGFR1 and p85α co-immunoprecipitation in different cell types. It is important to monitor these interactions in live cells, as cell lysing can show false interactions. The speed of protein movement and the percent of mobile molecules in live cells could be used to monitor direct or indirect interactions between proteins, as well as the formation of protein complexes and their association with cellular structures. We have used FRAP to study the mobility of p85α in the cytoplasm and nucleus of live human TE671 cells and to determine whether the interaction with FGFR1 will influence p85α mobility. Using TE671 medulloblastoma cells as a model, we demonstrate that the mobility of p85α-fused to enhanced green fluorescent protein (EGFP) is significantly reduced when cotransfected with FGFR1, in both the cytoplasm and nucleus. This effect was abolished by deletion of the tyrosine kinase domain from FGFR1 (the catalytic, signaling region of the receptor), even though it changed the mobile fraction of p85α-EGFP. We find FRAP to be a valuable technique for protein interaction studies and conclude that p85α mobility is regulated by cytoplasmic/nuclear FGFR1 in the cytoplasmic and nuclear compartments of live cells.

Introduction

Studying protein dynamics involves defining the interactions that a particular protein can be involved in, which are crucial for understanding a protein's function and regulation. Numerous techniques are used for such studies; genetic yeast two-hybrid screens and biochemical co-immunoprecipitation (co-IP) are two of the most common experimentation methods used to understand the specific associations of different proteins. Yeast two-hybrid studies are prone to a significant number of false positives. Additionally, in co-IP, in which a protein specific antibody is used to isolate protein complexes from cell lysates, false interactions may be observed when cells are lysed and proteins from different subcellular compartments are brought together. Therefore it is important to monitor protein interactions in live cells and formation of protein complexes in live, undisrupted cells may be evaluated using biophotonic techniques.[1] More recently, fluorescent resonant energy transfer (FRET) has been accepted as a suitable method for studying direct protein−protein interactions in live cells.[1−3] An association between proteins bearing fluorescent tags may be revealed by FRET, provided that the proteins directly interact with each other and the distance between their fluorescent tags is no more than 10 nm.

The speed of protein movement also could potentially be used to monitor direct and indirect interactions among proteins. The formation of complexes involves three-dimensional structural changes and movement of a larger structure through the same space as the individual protein once moved. Consequently, the speed of protein movement will be reduced. Proteins can also bind to immobile cellular structures, such as the cytoskeleton and nuclear matrix, which further influence cellular movement by immobilizing the molecule. Here, we demonstrate that measuring protein movements using fluorescence recovery after photobleaching (FRAP) can be used to monitor protein interactions and associations in live cells.

FRAP measures the diffusion coefficient and the mobile fraction of an ensemble of fluorescent particles. In this technique, fluorescent molecules within a small region of a cell are made nonfluorescent with a very high-intensity illumination (resulting in photochemical destruction or irreversible modification of fluorescent molecules) and the exchange between the bleached and unbleached populations of a fluorophore-linked protein is then monitored.[2,4,5] FRAP experiments originally started in the 1970s using lipophillic or hydrophilic fluorophores (i.e., fluorescein) coupled to proteins and lipids.[2,4] The discovery

† Part of the special issue "Gerald Small Festschrift".

* To whom correspondence should be addressed. E-mail: pnprasad@acsu.buffalo.edu.

§ Department of Pathology and Anatomical Sciences.

‡ Department of Chemistry.

10.1021/jp0400972 CCC: $27.50
Published on Web 06/30/2004

of green fluorescent protein (GFP), originally extracted from the jellyfish *Aequorea Victoria*, has increased the scope for this technique.[6] GFP molecules can be attached to a protein of interest with minimal effects on functionality. GFP molecules have good photostability at low intensity excitation but can be irreversibly bleached at higher excitation intensities, without damaging intracellular structures.[6] These properties of GFP have thus considerably enhanced the biological applications of photobleaching studies.

A major group of cellular signaling initiators are receptor tyrosine kinases (RTKs), which are membrane-spanning receptor molecules. The cellular signals generated by ligands binding to RTKs induce a variety of cellular changes, including cytoskeletal remodeling, cellular growth and differentiation, survival, and apoptosis. The signals originate at the membrane and are ultimately transmitted to the nucleus through multiple second messengers and kinases. In addition, some RTKs are released from cell membranes and translocate to the nucleus where they activate nuclear signaling proteins and/or gene transcription.[7−10] Fibroblast growth factor receptor-1 (FGFR1) is an RTK that is involved in cellular growth and differentiation, migration, and development. FGFR1 is associated with the plasma membrane in many cells. In addition, newly synthesized FGFR1 was shown to be released from endoplasmic reticulum membranes into the cytosol and subsequently translocate to the nucleus were it activates transcription of diverse genes.[9] FGFR1 is activated upon ligand binding, which induces autophosphorylation and dimerization resulting in the recruitment of a variety of proteins that serve as second messengers (i.e., Grb2, FRS2, PLC-γ, and Shc) and protein kinases that transduce signals to the nucleus.[11] An example of this type of RTK-activated kinase is cytoplasmic/nuclear phosphoinositide-3-kinase (PI3K). PI3K contains two subunits, an 85 kDa regulatory subunit (p85α) and a 110 kDa catalytic subunit (p110). Binding of the p85α subunit to an activated RTK triggers the activation of PI3K. Recent reports indicate that the effect of PI3K activity is necessary for FGFR1 cytoplasmic and nuclear signaling.[12−14] Further, other reports indicate an interaction of p85α (a subunit of PI3K) with FGFR1 in *Xenopus* embryos during gastrulation.[13]

In this study, we used FRAP to determine the mobility of p85α in the cytoplasm and nucleus of live human TE671 cells and investigate whether FGFR1 may influence p85α mobility. Using TE671 medulloblastoma cells as a model, we demonstrate that p85α-fused to enhanced green fluorescent protein (EGFP) has approximately 20-fold slower mobility than nonfused EGFP. Transfection of FGFR1 significantly reduced p85α-EGFP mobility in both the cytoplasm and nucleus. This effect was eliminated by deletion of the FGFR1 tyrosine kinase (TK) domain (the catalytic, signaling region of the receptor).

Materials and Methods

Cell Culture, Plasmids, and Transfection. Human TE671 medulloblastoma cells were grown in DMEM (Gibco) supplemented with 10% FBS and 1% penicillin−streptomycin (Invitrogen) and maintained at 37 °C with 5% CO_2 in a humidified incubator. Cells were kept in serum-free medium 24 h before transfection until the end of experiment.

TE671 were transfected using Lipofectamine 2000 (Invitrogen) according to manufacture's protocol. Seventy percent confluent TE671, plated 1 day prior to transfection on glass cover slips, were transfected with 5 μg of p85-EGFP, pcDNA3.1-FGFR1 and/or control pcDNA3.1 or pEGFP vectors. After 28 h, cells were harvested and lysed in lysis buffer (described below). Cells were analyzed via confocal microscopy and fluorescent recovery after photobleaching (FRAP) 24−30 h after transfection.

p85-EGFP was a kind gift from Sandra Marmiroli (Institute of Normal and Pathological Cytomorphology, Bologna, Italy). FGFR1 was generated by cloning the full length coding region of human FGFR1 cDNA into the pcDNA3.1 vector.[10] FGFR1-(TK-), lacking the tyrosine kinase domain, was generated by deleting the FGFR1 sequence 21 bp downstream from the transmembrane domain and inserted into the pcDNA3.1 vector.

Cell Lysis and Western ImmunoBlotting. Nuclear and cytoplasmic fractions were isolated and characterized as previously described.[15,16] Briefly, cells were lysed in buffer containing 1 mM $NaVO_3$, 10 μL/mL Protease Inhibitor Cocktail (Sigma), 25 mM NaF, 2 mM DTT, 1 μL/mL PMSF, 0.14% NP40 in 10 mM Hepes pH 7.5, 10 mM KCl, 0.1 mM EDTA, and 0.1 mM EGTA. The lysates were then centrifuged at 8000 rpm for 1 min and the supernatant, representing the cytoplasmic fraction with cytoplasmic membranes, was removed. The resulting nuclear pellet was washed in 1% Triton X buffer pH 7.4 containing 50 mM HEPES, 50 mM NaCl, 5 mM EDTA and protease inhibitors and briefly sonicated.

Protein content was then determined using the BioRad assay. For western immunoblotting, samples were heated at 95 °C for 10 min and equal amounts of protein loaded into 6−8% SDS−polyacrylamide gels, electrophoresed, and transferred to nitrocellulose membranes. In each experiment, equal protein loading was confirmed by Coomasie staining of the nontransferred portion of the gel. The membranes were then probed with the appropriate antibodies (EGFP (Clontech), McAb6,[17] and p85 (Upstate Biotechnology)

FRAP Setup. Excitation light was provided by the 488 nm line from an argon ion laser, in our FRAP setup (Figure 1). A galvanometer mirror (GSI Lumonics) was used to switch the laser beam into a low intensity imaging beam and high-intensity bleaching beam. In the imaging beam path, neutral density filters were used to lower the laser intensity. Both beam paths were combined by a beam splitter (30/70 splitter) and were coupled into a single mode fiber for delivery into the confocal microscope (BioRad MRC-1024). The BioRad time-course software was used for FRAP experiments and a trigger available from microscope controller in combination with a pulse generator was used to switch the imaging beam into the high-intensity bleaching beam. In this method, switching between the bleaching beam and the imaging beam can be done within a few milliseconds. The bleach pulse interval was variable from 10 ms to 10 s. Our confocal microscope was also modified to obtain a localized spectrum from different compartments of the cell being imaged. The details of the localized spectroscopy setup are described elsewhere.[19,20]

In our FRAP experiment, the laser beam was focused onto the slide using a 60×, 1.4 NA oil immersion objective. BioRad time-course software was used to select the FLASH area (photobleached area), and fluorescence recovery from selected areas of cells was monitored. The typical intensity used for imaging was around 20 μW, whereas the photobleaching intensity was around 5−6 mW. These intensity levels were found to be good enough for imaging and photobleaching with a 488 nm laser. The software control allowed us to choose reproducible small areas for photobleaching. For imaging EGFP fluorescence, a DF520/30 filter (Chroma Technology Corp.) was used. Localized emission spectra from cells were routinely acquired to confirm that there was no significant autofluores-

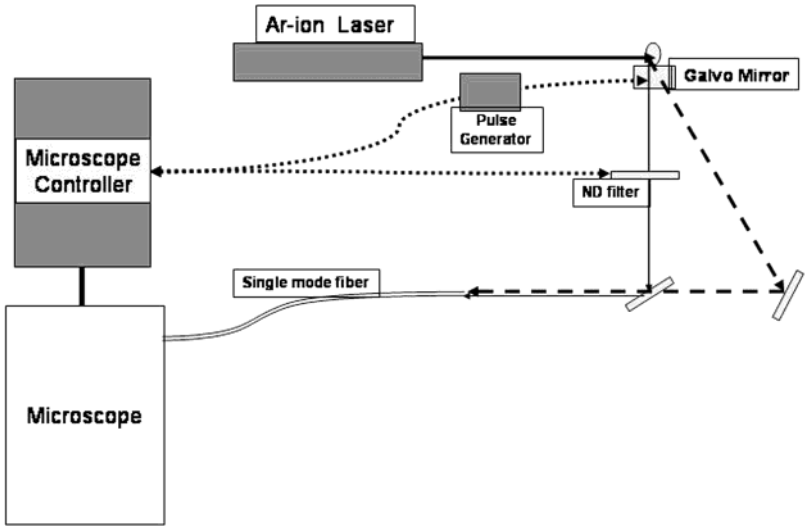

Figure 1. FRAP setup. 488 nm excitation provided by Argon ion laser lead to a galvanometer mirror, to switch laser beam intensity from low (20 μW) to high (5−6 mW) power. Neutral imaging filters where in the imaging path to lower laser beam intensity. A beam splitter (30/70 splitter) was combined the beams into a single mode fiber for delivery into a confocal microscope (Biorad MRC-1024), with the GFP filter (DF520/30). Images were acquired using time course software (Bio-Rad).

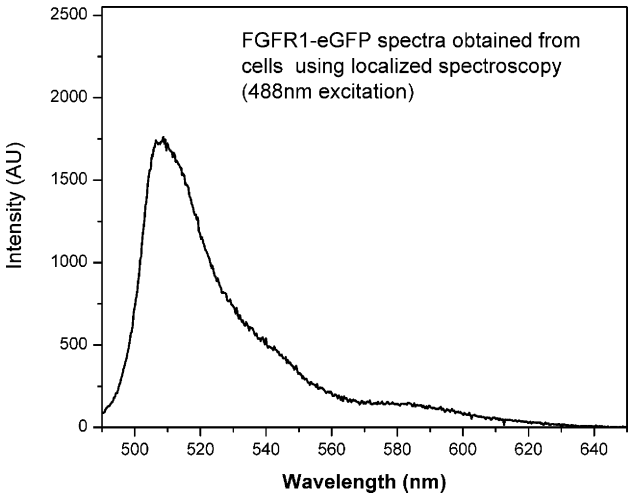

Figure 2. EGFP emission spectra. FGFR1-EGFP transfected TE671 cell emission spectra. EGFP peak can be seen at ≈510 nm, with some autofluorescence in the range of 560−580 nm that was omitted using specific filter sets.

cence, and that the emission observed was indeed from EGFP molecules (Figure 2).

Data Analysis. The acquired images were analyzed using "Image J" software (NIH). For each analysis ($n = 3$) three regions were chosen within each compartment, then averaged to estimate the compartment behavior within the bleached region. Regions chosen were of the same size (∼10 × 7 pixels, i.e., 6.5 μm × 4.5 μm area per region of interest). Data were corrected for background intensity and for the overall loss in total intensity as a result of the bleach pulse and the imaging scans (Figure 3). Recovery measurements were quantified by fitting normalized fluorescence intensities of bleached areas to a one phase exponential association by using the nonlinear regression algorithm in GraphPad software (Prism); this program was also used for plotting data and statistical analysis. The analyses were repeated several times, and the results presented are representative of several cells.

Results

p85α and FGFR1 Subcellular Distribution. Endogenous p85α is found in both the cytoplasm and nucleus (Figure 4A)

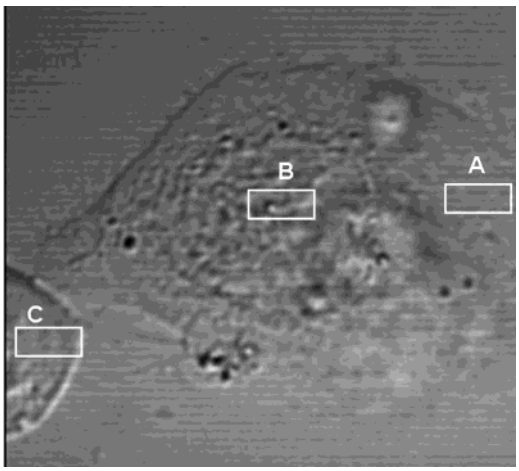

Figure 3. Compartment identification. A transmission image was acquired for each cell analyzed and used to identify each compartment. For each analysis ($n = 3$) three regions were chosen within each compartment and then averaged to estimate the compartment behavior within the bleach region. Regions chosen were of the same size (10 × 7 pixels per region of interest). Examples of selected regions are indicated in the image: (A) cytoplasm; (B) nuclear interior; (C) background.

of TE671 cells. The p85α-EGFP fusion protein was verified via western immunoblots of total cell lysates [Figure 4B; the same p85α-EGFP band was observed with anti-p85α antibody (not shown) and distribution confirmed via confocal microscopy. FGFR1 is also located in both the cytoplasmic and nuclear fractions of TE671 cells upon FGFR1 transfection, with only trace levels naturally expressed (Figure 4C). Western blot analysis of FGFR1 revealed the presence of different degrees of glycosylation (Figure 4C), corresponding to the following sizes: 103, 118 and 145 kDa, which has been previously shown by Stachowiak et. al.[15,21,22]

Subcellular Compartmental Comparison of p85α's Mobility. Fluorescent recovery after photobleaching (FRAP) provides information about the mobility and stability of cellular structures and proteins.[23] The mobile fraction varies upon the environmental conditions that it is under; i.e., protein interactions, associations with membranes, cytoskeleton, or nuclear matrix markedly slow protein mobility by restricting free

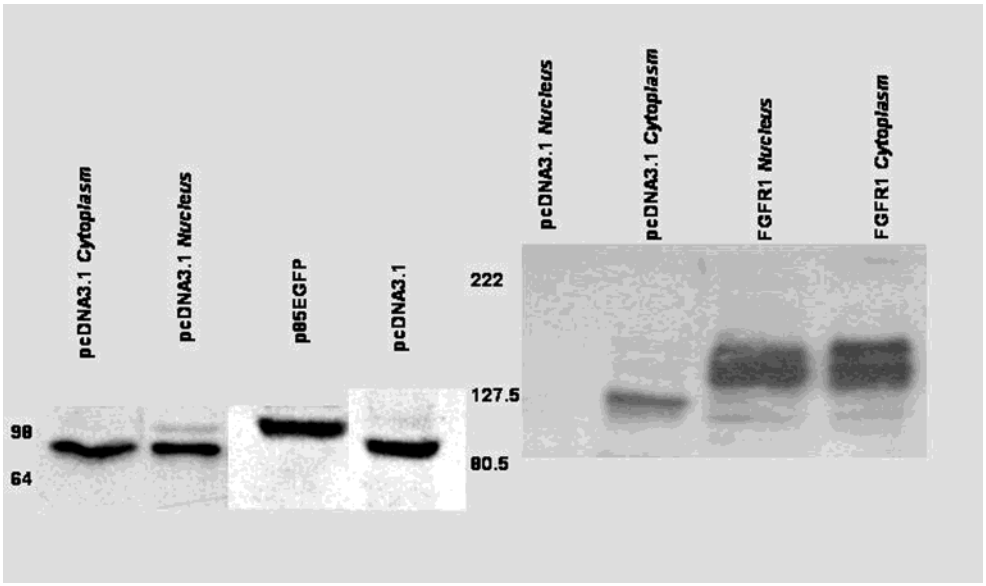

Figure 4. Cellular distribution of p85α and FGFR1. TE671 cells were transfected with 5 μg p85α-EGFP or pcDNA3.1-FGFR1 and the cytoplasmic and nuclear fractions isolated. Nitrocellulose membranes probed with (A) p85α specific antibody (Upstate Technology), (B) EGFP antibody (Clontech), and (C) FGFR1 antibody. Expression of endogenous nuclear FGFR1 was observed only after prolonged film exposure (not shown; 19). The HRP conjugated secondary antibody (Pierce) was exposed using a Chemiluminescence kit (Pierce) following manufacturers instructions

diffusion.[24] Strong associations with cellular structures also immobilize cellular proteins and thereby reduce the size of their mobile pool.[25] FRAP was utilized in this study to further characterize the movement of p85α, with the first aim being to determine if there is a difference between cytoplasmic and nuclear p85α mobility.

To determine the mobility of p85α in cellular compartments, TE671 cells expressing p85α-EGFP were monitored with a confocal laser scanning microscope. A rectangular region across the width of a living cell was bleached with a high-powered laser pulse and fluorescent recovery (i.e., p85α movement) was monitored over time with sequential imaging scans (Figure 5A). p85α-EGFP was cotransfected with pcDNA3.1, which is an empty vector that only expresses a neomycin resistance gene, to control for overall amount of DNA transfected. This did not influence the mobility of p85α-EGFP (data not shown). Monitoring was conducted until fluorescence reached a steady state (Figure 5B). To assess protein mobility and recovery, paraformaldehyde-fixed cells expressing EGFP were monitored to ensure that bleaching was irreversible (Figure 5D). As a control for a freely diffusible protein, cells expressing EGFP alone were used and they exhibited very fast FRAP kinetics ($t_{1/2} < 0.2$ s; Table 1), which exceeded the detection limits of our experimental recording settings (Figure 5C). The recovery half-time of p85α, comparable in both cellular compartments analyzed, was 2.629 s in the cytoplasm and 2.027 s in the nucleus (Table 1). Therefore, p85α's movement is more restricted than that of EGFP. The mobile population of p85α within the cytoplasm was 91.55% of the prebleached fluorescence intensity corrected for the loss of fluorescence caused by scanning, whereas it was significantly reduced within the nucleus to 76.53% ($p < 0.0074$; two tailed *t*-test; Table 2 and Figure 5B).

Attenuation of p85α Mobility in the Presence FGFR1. To test if protein interactions influence the mobility of p85α, FGFR1 was cotransfected with p85α-EGFP. p85α's mobility rate was significantly attenuated in both the cytoplasm ($p < 0.0002$, two-tailed *t*-test) and nucleus ($p < 0.0011$; two tailed *t*-test), with the recovery half-time increasing to greater than 10 s (Figure 6, Table 1). As observed with p85α alone, there is no significant difference between the mobility rates observed in the cytoplasm and nucleus of the cell in the presence of FGFR1 (Table 1). The mobile population of p85α within the cytoplasm was significantly lower ($p < 0.0008$, two tailed *t*-test) in the presence of FGFR1, 75% of the prebleached fluorescence intensity corrected for the loss of fluorescence caused by scanning (Table 2 and Figures 5B and 6). There was no significant difference in mobility within the nucleus.

To test whether active FGFR1 is required for the observed effects on p85α mobility an inactive FGFR1(TK-) mutant was used. The FGFR1(TK-) mutant lacks the tyrosine kinase domain and therefore cannot propagate signals into the cell. In this case, we found no significant change in the recovery time for p85α-EGFP. However, there was a significant difference in the mobile population of p85α in the presence of FGFR1(TK-). The mobile population within the cytoplasm was significantly reduced ($p < 0.0001$, two tailed *t*-test) to 59.75% of the prebleached fluorescence intensity corrected for the loss of fluorescence caused by scanning and 36.94% within the nucleus. A significant difference ($p < 0.0004$, two tailed *t*-test) could also be observed in comparing the nucleus to the cytoplasm in the presence of FGFR1(TK-) (Table 2, Figure 6B).

Discussion

The present study has shown that both cytoplasmic and nuclear p85α reside in immobile and mobile pools, with the majority representing mobile pools that undergo protein movement-dependent recovery after photobleaching. The mobility rate of the p85α mobile pools were over 20-fold greater than the EGFP alone, which correlates with the larger size of p85α-EGFP. It may also reflect its complex interactions with cellular proteins.

The presence of FGFR1 increased the recovery time of p85α approximately 5-fold. Transfected FGFR1 was shown to increase synthesis of its ligand FGF-2 and to co-accumulate with FGF-2 in the cell nucleus, which demonstrate that transfected FGFR1 becomes activated and signals similar to stimulated, endogenous FGFR1.[9] The potential interaction of FGFR1 and p85α in *Xenopus* oocytes has been indicated by co-immunoprecipitation[13] and their co-association with cellular

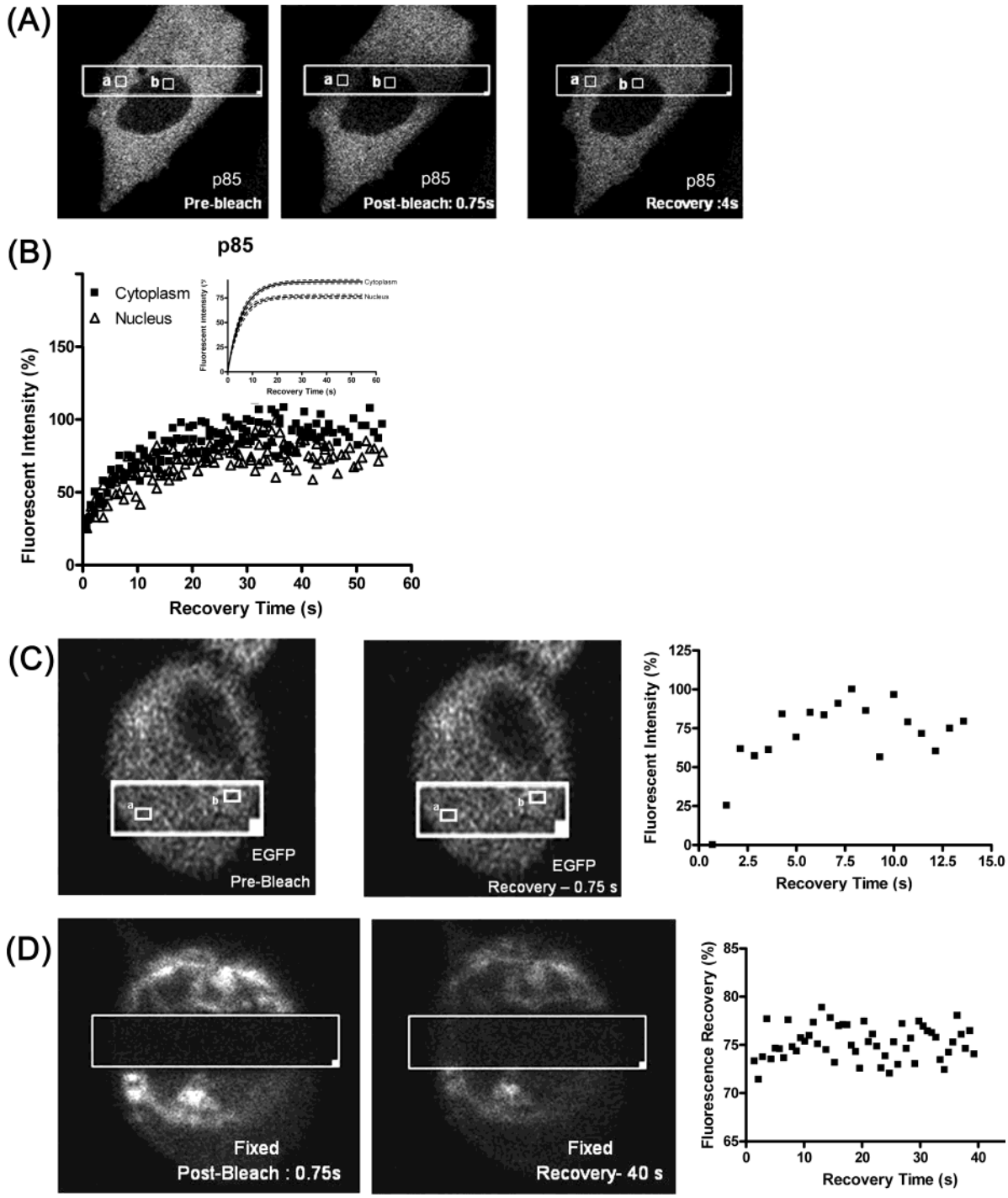

Figure 5. p85α mobility. (A) p85α-EGFP with pcDNA3.1 (empty vector) distribution and bleach area. "a" and "b" indicate cytoplasm and nucleus, respectively. (B) p85α-EGFP recovery time. Inset plot shows the 95% confidence recovery curves. (C) EGFP recovery time. (D) Paraformaldehyde fixed cell recovery time. Photobleaching was accomplished with a 0.75 s high powered bleach pulse (5−6 mW), and images were acquired with low powered (20 μW) scanning at indicated times. Recovery times are given in Table 1.

membranes and localization within similar intranuclear domains has been revealed by immunostaing of fixed cells.[22,26] Consistent with this, we found attenuation of p85 movements by FGFR1 and this attenuation required the presence of the tyrosine kinase domain in FGFR1. This tyrosine kinase domain acts both as catalytic (phosphorylating) domain and the domain to which p85α and other signaling proteins bind. Thus, the reduced recovery rate is, presumably, at least in part, due to binding of p85α to FGFR1. The FGFR1-induced decrease in the rate of p85α mobility could also reflect, in part, a p85α conformational change due to binding to p110[18] and other proteins.

In addition, FGFR1 may increase p85α association with the extranuclear cytoskeleton, as indicated by the decrease in the mobile population of p85α in the presence of FGFR1. Approximately 28% of nuclear p85α-EGFP resided in an immobile pool, which is in contrast to a 100% mobile EGFP population. The size of the nuclear p85α immobile pool was larger than in the cytoplasm, consistent with p85α interaction with nuclear matrix.[26] The nuclear mobile pool of p85α was not affected by FGFR1, but it was markedly reduced by inactive FGFR1(TK-). FGFR1(TK-) is known to act as a dominant negative mutant that forms inactive dimers with endogenous FGFR1 and thus

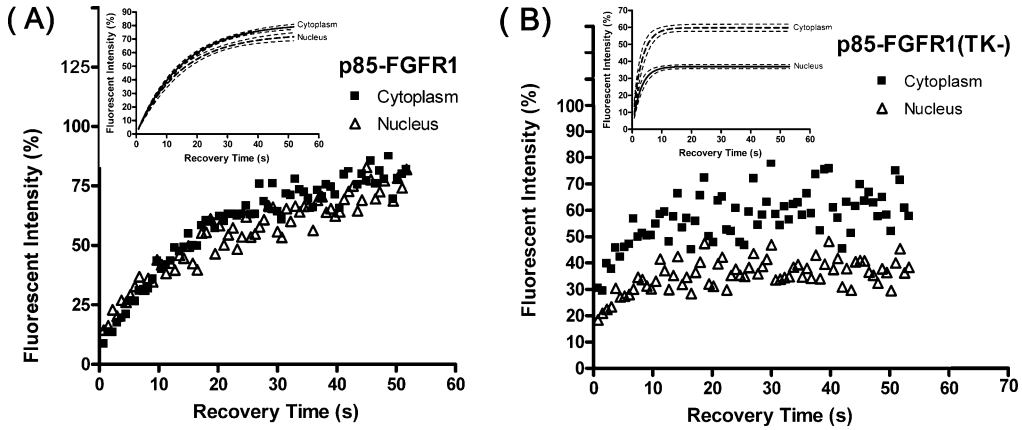

Figure 6. FGFR1 tyrosine kinase domain attenuates p85's movement. Equal amounts of FGFR1 and p85-EGFP or FGFR1(TK-) and p85-EGFP were transfected into TE671 cells. Recovery curve and 95% confidence interval for (A) p85-EGFP-FGFR1 and (B) p85-EGFP-FGFR1(TK-). Photobleaching was accomplished with a 0.75 s high powered bleach pulse, and images were acquired with low powered scanning. Data were acquired from best-fit curves (GraphPad) ($n = 3$), and recovery times are given in Table 1.

TABLE 1: FGFR1 Influences p85's Recovery Time[a]

transfected plasmids	cytoplasm ($t_{1/2}$, s)	nucleus ($t_{1/2}$, s)
p85α EGFP-pcDNA3.1	2.629 ± 0.292	2.027 ± 0.279
p85α EGFP-pFGFR1	10.50 ± 1.03	10.08 ± 1.70
p85α EGFP-pFGFR1(TK-)	2.515 ± 0.802	2.249 ± 0.692
pEGFP	0.143 ± 0.131	0.083 ± 0.08

[a] Plasmids: pEGFP expresses nonfused EGFP; p85α-EGFP expresses fused p85α-EGFP protein; pcDNA3.1 = control plasmid; pFGFR1 expresses full length FGFR1; pFGFR1(TK-) expresses tyrosine kinase-deleed FGFR1. $t_{1/2}$ for p85-EGFP, p85EGFP-FGFR1, p85αEGFP-FGFR1(TK-), and EGFP are given. Photobleaching was accomplished with a 0.75 s high powered bleach pulse and images were acquired with low powered scanning. Data acquired from best-fit cures ($n = 3$) (GraphPad). Standard deviation given for each recovery half-time.

TABLE 2: FGFR1 Influences p85's Mobility[a]

transfected plasmids	cytoplasm (% mobile)	nucleus (% mobile)
p85α EGFP-pcDNA3.1	91.55 ± 2.01	73.53 ± 1.97
p85α EGFP-pFGFR1	81.66 ± 2.76	73.8 ± 4.08
p85α EGFP-pFGFR1(TK-)	59.75± 2.08	36.94 ± 1.21
pEGFP	93.29 ± 1.01	100 ± 1.42

[a] Plasmids are described in Table 1. Mobile fraction for p85-EGFP, p85EGFP-FGFR1, p85EGFP-FGFR1(TK-), and EGFP. Data acquired from best-fit cures ($n = 3$) (GraphPad). Standard deviation given for each mobility.

blocks their functions.[9,22] Here in TE671 cells the increase of the p85α immobile pool by FGFR1(TK-) likely reflects the inhibition of endogenous FGFR1, which prevents the activation of p85α. The immobilization induced by the expression of FGFR1(TK-) is presumably due to p85α binding to stationary cellular structures, such as the nuclear matrix and cytoskeleton. An interesting finding in this experiment is that the mobility of p85α was less affected by FGFR1(TK-) in the cytoplasm than in the nucleus, which might be due to higher levels of endogenous FGFR1 in the cytoplasm.

On the basis of the obtained results, we conclude that a low level of endogenous FGFR1 signaling is necessary to maintain the majority of p85α in the mobile nuclear pool, whereas increased FGFR1 synthesis decelerates the movement of the mobile p85α pool. Number functions have been described for nuclear FGFR1[9] and nuclear p85α[26] of which several are overlapping, including molecular scaffolding and DNA and RNA synthesis and processing. Regulation of the size of the nuclear p85α mobile pool and the speed of its movements by FGFR1, shown in this study, further indicate that these two proteins act in concert to control diverse nuclear functions.

In conclusion, we show that FRAP can be used to study cellular signaling that involves changes in protein−protein interactions and help in dissecting signaling pathways. The present work shows that FGFR1 signaling regulates p85α distribution between immobile and mobile cellular pools and attenuates the mobility rate of p85α. Elucidation of the exact mechanisms and interacting factors that cause the increase in p85α recovery time and the exact nature of its immobile pools require further studies.

Acknowledgment. This study was supported in part by AFOSR (P.N.P.), grants from NSF (IBN-9728923), NIH (NS43621-01), the American Parkinson Disease Association, and from John R. Oishei Foundation to M.K.S. S.M.D. was supported by an IGERT fellowship from NSF (DGE-9870668).

References and Notes

(1) *Introduction to Biophotonics*; Prasad, Paras N., Ed.; Wiley-Interscience: New York, 2003.
(2) Axelrod, D.; Koppel, D.; Schlessinger, J.; Elson, E.; Webb, W. *J. Biophys.* **1976**, *16*, 1055.
(3) Day, R. N. *Mol. Endocrinol.* **1998**, *12*, 1410.
(4) Edidin, M.; Zagyansky, Y.; Lardner, T. *Science* **1976**, *191*, 466.
(5) Lippincott-Schwartz, J.; Snapp, E.; Kenworthy, A. *Nat. Rev. Mol. Cell Biol.* **2001**, *2*, 444.
(6) Swaminathan, R.; Hoang, C. P.; Verkman, A. S. *Biophys. J.* **1997**, *72*, 1900.
(7) Lin, S.; Makino, K.; Xia, W.; Matin, A.; Wen, Y.; Kwong, K.; Bourguignon, L.; Hung, M. *Nat. Cell Biol.* **2001**, *3*, 802.
(8) Marti, U.; Ruchti, C.; Kampf, J.; Thomas, G. A.; Williams, E. D.; Peter, H. J.; Gerber, H.; Burgi, U. *Thyroid* **2001**, *11*, 137.
(9) Stachowiak, M. K.; Fang, X.; Myers, J. M.; Dunham, S. M.; Berezney, R.; Maher, P. A. 11. Stachowiak, E. K. *J. Cell Biochem.* **2003**, *90*, 662.
(10) Stachowiak, E. K.; Maher, P. A.; Tucholski, J.; Mordechai, E.; Joy, A.; Moffett, J.; Coons, S.; Stachowiak, M. K. *Oncogene* **1997**, *14*, 2201.
(11) Klint, P.; Claesson-Welsh, L. *Frontiers Biosci.* **1999**, *4*, 165.
(12) Browaeys-Poly, E.; Cailliau, K.; Vilain, J. *Eur J Biochem.* **2000**, *267*, 6256.
(13) Ryan, P. J.; Paterno, G. D.; Gillespie, L. L. *Biochem. Biophys. Res. Commun.* **1998**, *244*, 763.
(14) Klingenberg, O.; Wiedlocha, A.; Olsnes, S. *J. Biol. Chem.* **2000**, *275*, 11972.
(15) Stachowiak, M. K.; Maher, P. A.; Joy, A.; Mordechai, E.; Stachowiak, E. K. *Mol. Biol. Cell* **1996a**, *7*, 1299.
(16) Stachowiak, M. K.; Maher, P. A.; Joy, A.; Mordechai, E.; Stachowiak, E. K. *Mol. Brain Res.* **1996b**, *38*, 161.
(17) Hanneken, A.; Maher, P. A.; Baird, A. *J. Cell Biol.* **1995**, *128*, 1221.
(18) Fruman, D. R.; Meyers; Cantley, L. *Annual Rev. Biochem.* **1998**, *67*, 481.

(19) Pudavar, H. E.; Kapoor, R.; Wang, X.; Prasad, P. N. *Symposium on Biophotonics and Nanomedicine*; Buffalo, NY, 2000.

(20) Wang, X.; Pudavar, H.; Kapoor, R.; Krebs, L.; Bergey, E.; Liebow, C.; Prasad, P.; Nagy, A.; Schally, A. *J. Biomed. Opt.* **2001**, *6*, 319.

(21) Myers, J. M.; Martins, G. G.; Ostrowski, J.; Stachowiak, M. K. *J. Cell Biochem.* **2003**, *88*, 1273.

(22) Peng, H.; Myers, J.; Fang, X.; Stachowiak, E. K.; Maher, P. A.; Martins, G. G.; Popescu, G.; Stachowiak, M. K. *J. Neurochem.* **2002**, *81*, 506.

(23) Mistelli, T. *Science* **2001**, *291*, 843.

(24) Edidin, M.; Zuniga, M. C.; Sheetz, M. P. *Proc. Natl Acad. Sci. U.S.A.* **1994**, *91*, 3378.

(25) Maruvada, P.; Baumann, C. T.; Hager, G. L.; Yen, P. M. *J. Biol. Chem.* **2003**, *278*, 12425.

(26) Martelli, A.; Tabellini, G.; Borgatti, P.; Bortul, R.; Capitani, S.; Neri, L. M. *J. Cell. Biochem.* **2003**, *88*, 455.